RPA – Tool for Rocket Propulsion Analysis

A. Ponomarenko

http://www.propulsion-analysis.com

contact@propulsion-analysis.com

Abstract

This paper presents the Rocket Propulsion Analysis tool (RPA) - a multi-platform computational package intended for use in the conceptual and preliminary design of liquid-propellant rocket engines.

A description of the components and the most important aspects of the physical modeling is included. It provides details on the following modules: thrust chamber performance analysis, combustion chamber sizing and nozzle contour design, thrust chamber thermal analysis, engine cycle analysis and weight estimation. Physical models implemented in RPA enable the analysis of rocket engines with accuracy sufficient for conceptual and preliminary design studies.

All modules are integrated into executable with user-friendly graphical user interface.

Development tools (set of libraries and documented API) are available, allowing the user to create various custom solutions, including simple scripts written in JavaScript, programs written in Python, or complex applications written in C++.

Introduction

Rocket Propulsion Analysis tool (RPA) is a commercially available multi-platform computational package intended for use in the conceptual and preliminary design of liquid-propellant rocket engines.

The motivation of RPA development was to:

- provide modern multi-platform tool for prediction of rocket engine performance at the conceptual and preliminary stages of design,
- capture impacts on engine performance due to variation of design parameters,
- assess the parameters of main engine components (thrust chamber, turbopump, gas generator/preburner) to provide better data for detailed analysis/design,
- assist in education of new generation of propulsion engineers.

The developed code features the following characteristics:

- steady-state analysis,
- simplified model initialization with minimum of input parameters,
- wide usage of semi-empirical relations and coefficients.

Modules

The package provides a seamless integration of several modules to perform:

- obtaining the thermodynamic properties of propellant components, thermodynamic and transport properties of combustion products, thermodynamic analysis of combustion process, and thrust chamber performance analysis,
- combustion chamber sizing and nozzle contour design,
- thrust chamber thermal analysis,
- engine cycle analysis and weight estimation.

Implemented physical models, numerical methods, and algorithms allow the rapid estimation of design parameters of propulsion systems with accuracy sufficient for conceptual and preliminary design studies, as well as for rapid evaluation of different variants of the propulsion systems.

Thermodynamics and thrust chamber performance analysis

RPA utilizes expandable thermodynamic data library mainly based on NASA Glenn thermodynamic database [4],[5], which contains data for both reaction products and reactants (propellant components). Properties for most of the liquid propellant components used for rockets applications are available, including (but not limited to) liquid hydrogen, RP-1, RG-1, T-1, synthine, liquid methane, hydrazine, MMH, UDMH, methyl alcohol (concentrated and water solutions), liquid oxygen, nitrogen tetra-oxide, hydrogen peroxide (concentrated and water solutions), and others.

Additional physical properties of the liquid propellant components required for thermal and engine cycle analyses (such as density, viscosity, thermal conductivity, and heat of evaporation) are provided in the form of a 2D property tables (p,T), and obtained using interpolation. Properties for many of the liquid propellant components are

available, including liquid hydrogen, RP-1, T-1, liquid methane, hydrazine, MMH, UDMH, methyl alcohol (concentrated), liquid oxygen, nitrogen tetra-oxide.

Both data libraries are stored as ASCII file, and can be modified by the user either with a provided thermodynamic database editor, or in any text editor. User-defined propellant components and/or combustion products can be easily added.

The tool implements a thermodynamic analysis module which utilizes a free energy minimization approach to obtain the combustion composition for given propellant components and combustion conditions: *(p,I)=const* for combustion chamber, and *(p,S)=const* for nozzle flow. Detailed description of used physical models is available in [1].

The following assumptions are made for the calculation of the ideal thrust chamber performance (in terms of specific impulse I_{sp}):

- adiabatic, isenthalpic combustion in combustion chamber,
- adiabatic, isentropic (frictionless and no dissipative losses) quasi-one-dimensional nozzle flow for both shifting and frozen equilibrium models,
- ideal gas law,
- no dissipative losses.

To obtain the rocket performance, the program calculates conditions at several stations of the thrust chamber. It always includes the calculation of combustion parameters at injector face, nozzle throat, and nozzle exit section, defined by either nozzle exit pressure p_e , expansion pressure ratio p_c/p_e , or expansion area ratio A_e/A_t .

The user can force the program to calculate the performance with respect of stagnation pressure drop between injector face and nozzle inlet, defining such parameters as a chamber mass flux or a nozzle inlet contraction area ratio A_c/A_t .

Default nozzle flow model is a shifting equilibrium: combustion products continue to react and reach chemical equilibrium at each temperature and pressure conditions along the nozzle. The user can trigger the "freezing" of nozzle flow composition downstream of the throat. In this case, it is assumed that composition is "frozen" (infinitely slow reaction rates) during expansion along the nozzle. The location of "freezing" nozzle station is defined by either pressure ratio p_t/p_{fr} , or area ratio A_{fr}/A_t .

Detailed description of physical models used to obtain the ideal performance is available in [1].

Although the tool was actually intended for analysis of liquid propulsion systems, it can also be used for the thermodynamic analysis and performance prediction both solid and hybrid rocket engines. RPA obtains the proper combustion composition from any type of solid/hybrid propellants, including metalized ones.

RPA allows the user to estimate the performance of a throttled chamber, as well as performance at specific ambient pressure.

The software provides an integrated nested analysis tool to evaluate the performance at different conditions, stepping of up to four independent variables: component ratio, chamber pressure, nozzle inlet conditions, nozzle exit conditions.

The program is capable of predicting the delivered performance of thrust chamber using semi-empirical relations to obtain performance correction factors, including:

- performance loss due finite rate kinetics in combustion chamber and nozzle,
- divergence loss,
- performance loss due to finite-area combustion area,
- multi-phase flow loss,
- performance change due to nozzle flow separation,
- performance change due to thrust throttling.

Detailed description of used relations to obtain performance correction factors is available in [2].

Thrust chamber sizing

Thrust chamber sizing module is used to obtain the geometry parameters of the combustion chamber and the nozzle.

For thrust chamber sizing, the program provides three options:

- sizing for required thrust level at a specific ambient pressure,
- sizing for a specific propellant mass flow rate through the thrust chamber,
- sizing for a specific nozzle throat diameter.

The size of combustion chamber and the shape of nozzle inlet contour are defined parametrically by specifying such parameters as mass flux at nozzle inlet or chamber contraction area ratio A_c/A_t , chamber length L_c or characteristic length L^* , contraction half-angle b , relative parameters R_1/R_t , R_2/R_2^{max} , and R_n/R_t as shown in the Fig.1.

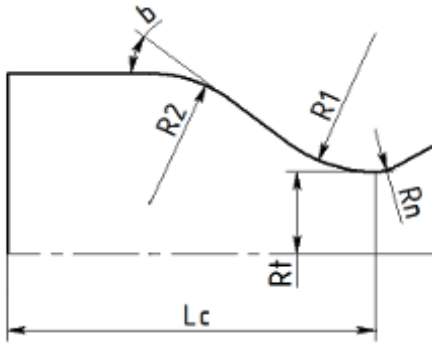

Fig. 1: Parametric design of nozzle inlet contour

For supersonic nozzle contour design, the program provides three options:

- cone nozzle with a specified exit half-angle,
- parabolic nozzle contour with specified or automatically assessed initial and/or exit half-angle,
- truncated ideal contour (TIC) with fixed expansion area ratio A_e/A_t and nozzle length L_e ,
- TIC with maximum thrust at fixed expansion area ratio A_e/A_t ,
- TIC with maximum thrust at fixed nozzle length L_e .

Nozzle with TIC is designed using axisymmetric method of characteristics (MOC).

To obtain the contour with the maximum thrust at specified conditions (A_e/A_t or L_e), the method of direct optimization is used. For this purpose, the program builds a set of ideal nozzle contours with exit Mach number in the range $M_e=(M_e)_{1D}...2(M_e)_{1D}$ where $(M_e)_{1D}$ is exit Mach number for quasi-one-dimensional nozzle flow, and then truncates them as specified. For each truncated contour, the thrust coefficient in vacuum is calculated as follows:

$$C_f = (C_f)_{2D}\ (1-\zeta_f)$$

where $(C_f)_{2D}$ is a thrust coefficient obtained for axisymmetric two-dimensional nozzle flow with known distribution of characteristic Mach number λ at nozzle exit section (see Fig.2) as given in [6]:

$$(C_f)_{2D} = 2\frac{A_e}{A_t}\int_0^1 \left(1-\frac{\gamma-1}{\gamma+1}\lambda^2\right)^{\frac{1}{\gamma-1}}\left[1+\lambda^2\frac{\gamma(2\cos^2\beta-1)+1}{\gamma+1}\right]\bar{r}\,d\bar{r}$$

and ζ_f is a correction factor due to wall friction in boundary layer as given in [7]:

$$\zeta_f = 1 - \frac{2\bar{\delta}_e^{**}}{1+\frac{1}{\gamma M_e^2}}$$

with relative momentum thickness given by $\bar{\delta}_e^{**}=\delta^{**}/R_e$, and momentum thicknessis δ^{**} for turbulent boundary layer given by [7]

$$\delta^{**} = \frac{\left(\frac{2}{\gamma-1}\right)^{0.1}}{\mathrm{Re}_{w_0}^{0.2}}\left(\frac{0.015}{\bar{T}_w^{0.5}}\right)^{0.8}\frac{\left(1+\frac{\gamma-1}{2}M_{we}^2\right)^{\frac{\gamma+1}{2(\gamma-1)}}}{M_w^{\nu+1}}\frac{\bar{S}^{0.2}}{\bar{r}_e^2}\times \left[\int_0^{\bar{S}}\frac{\bar{r}^{1.25}M^{1+1.25\,\nu}}{\left(1+\frac{\gamma-1}{2}M_w^2\right)^{\frac{1.36\,\gamma-0.36}{\gamma-1}}}d\bar{S}\right]^{0.8}$$

Relative wall temperature $\bar{T}_w = T_w/T^0$ is specified by user as an input parameter. All other parameters are obtained from quasi-one-dimensional thermodynamic analysis and axisymmetric MOC analysis.

Detailed description of used relations to obtain the thrust coefficient for nozzle with truncated ideal contour is available in [2].

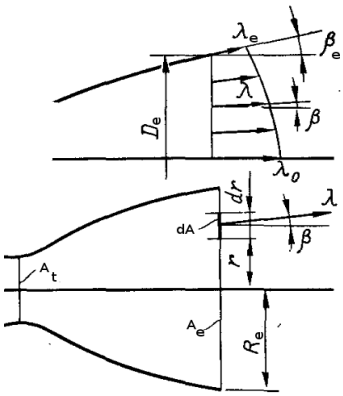

Fig. 2: Velocity field distribution at nozzle exit

From obtained set of contours, the table $C_f=f(A_e/A_t)$ or $C_f=f(L_e)$ is formed. The point C_f^{max} is found as an extremum of interpolated function, and then used to build the resulting contour.

Finally, the program estimates divergence efficiency $\eta_{\mathrm{div}}=1-(C_f)_{2D}/(C_f)_{1D}$ (where $(C_f)_{1D}$ is a thrust coefficient calculated for quasi-one-dimensional nozzle flow), drug efficiency $\eta_{drug}=1-\zeta_f$ and thrust coefficient C_f .

The designed thrust chamber contour can be exported in drawing interchange file format (DXF).

Thrust chamber thermal analysis

Thrust chamber thermal analysis module is capable of analyzing the heat transfer distribution (convective and radiation) and estimating the efficiency of the chamber cooling with any of the following cooling methods:

- radiation cooling,
- regenerative cooling (coaxial shells, welded tubes, or milled channels),
- film cooling,

– thermal barrier coating.

To estimate the hot gas side convective heat flux, the following methods can be used:

– Bartz method,
– Ievlev method,
– combined method, averaging results obtained from Bartz and Ievlev methods.

Detailed description of relations and methods used for thermal analysis is available in [3].

Convective heat transfer: Bartz method

The hot gas side convective heat flux is assessed by following equation:

$$q_w = \alpha_T (T_{aw} - T_w)$$

where adiabatic wall temperature is calculated by [8]

$$T_{aw} = T_c^0 \left[\frac{1 + Pr^{1/3} \left(\frac{\gamma - 1}{2} \right) M^2}{1 + \left(\frac{\gamma - 1}{2} \right) M^2} \right]$$

and the heat transfer coefficient is obtained from the following correlation [8]:

$$\alpha_T = \left[\frac{0.026}{D_t^{0.2}} \frac{(\mu_\infty^0)^{0.2} c_{p\infty}^0}{(Pr_\infty^0)^{0.6}} \left(\frac{p_c^0}{c^*} \right)^{0.8} \left(\frac{D_t}{R} \right)^{0.1} \right] \left(\frac{A_t}{A} \right)^{0.9} \sigma$$

The correction factor σ is given by [8]

$$\sigma = \left[\frac{1}{2} \frac{T_w}{T_c^0} \left(1 + \frac{\gamma - 1}{2} M^2 \right) + \frac{1}{2} \right]^{-0.68} \left[1 + \frac{\gamma - 1}{2} M^2 \right]^{-0.12}$$

All required parameters are obtained from quasi-one-dimensional thermodynamic analysis.

Convective heat transfer: Ievlev method

Ievlev obtained the hot gas side heat flux calculation method from integral boundary layer equations and semi-empirical heat transfer relations.

The hot gas side convective heat flux is assessed by following equation [6]:

$$q_w = \alpha_T \rho_x w_\infty (I_\infty^0 - I_w)$$

The heat transfer coefficient is calculated by [6]

$$\alpha_T = \frac{\left(\frac{z}{z_T} \right)^{0.089 Pr^{-0.56}} \left(1 - 0.21 \frac{1 - Pr}{Pr^{4/3}} \frac{\beta^2}{1 - \bar{T}_w} \right)^{0.9225}}{\left(307.8 + 54.8 \log^2 \left(\frac{Pr}{19.5} \right) \right) Pr^{0.45} z^{0.08} - 650}$$

where

$$\frac{z_T}{z} = \left(1.769 \frac{1 - \beta^2 + \beta^2 \left(1 - 0.08696 \frac{1 - \beta^2}{1 - \bar{T}_w + 0.1\beta^2} \right)}{1 - \bar{T}_w + 0.1\beta^2} \right)^{0.54}$$

$$z_T = \frac{\mathrm{Re}_0}{(1 - \gamma) \bar{D}^{\frac{1}{1-\gamma}} (I_\infty^0 - I_w)^{\frac{1}{1-\gamma}}} \times \int_{l_0}^{l} \frac{\rho_x}{\rho_\infty^0} \frac{\mu_\infty^0}{\mu_x} \bar{D}^{\frac{1}{1-\gamma}} (I_\infty^0 - I_w)^{\frac{1}{1-\gamma}} \beta \frac{d\bar{l}}{\cos\theta} + const$$

$$\beta = w / \sqrt{2\gamma (RT)_\infty^0 / \gamma - 1} \quad , \quad \bar{D} = d / d_t \quad , \quad l = l / d_t$$

$$\bar{T}_w = T_w / T_e \quad , \quad T_e = R T_\infty^0 / R_{1500} \quad ,$$

$$\frac{\rho_x}{\rho_\infty^0} = \frac{p}{p_c^0} \left(\frac{1 + \bar{T}_w}{2} - \frac{\beta^2}{4} \right)^{-0.823} \left(\frac{3 + \bar{T}_w}{4} - \frac{9\beta^2}{16} \right)^{-0.177}$$

$$\frac{\mu_\infty^0}{\mu_x} \approx \left(\frac{1 + \bar{T}_w}{2} - \frac{\beta^2}{4} \right)^{-0.7}$$

and R_{1500} is a gas constant of reaction products at T=1500 K.

The following approach is used to calculate the value $(I_\infty^0 - I_w)$ (as suggested in [9]):

for $T_\infty^0 > 1500\,K$ and $T_w < 1500\,K$:

– I_∞^0 is calculated as a stagnation enthalpy in combustion chamber,
– I_w is calculated as an enthalpy of reaction products at the temperature T_w, but with composition that corresponds to the temperature 1500 K;

for $T_\infty^0 > 1500\,K$ and $T_w > 1500\,K$:

– I_∞^0 is calculated as a stagnation enthalpy in combustion chamber,
– I_w is calculated as an enthalpy of reaction products at the temperature T_w.

All required thermodynamic and transpot parameters are obtained from quasi-one-dimensional thermodynamic analysis.

Radiation heat transfer

For given hot gas temperature in the core flow T_∞ and wall temperature T_w, the basic correlation for the radiation heat transfer (under some assumptions mentioned in [6]) is given by

$$q_r = \varepsilon_e \sigma \left(\varepsilon_r^{T_\infty} T_\infty^4 - \varepsilon_r^{T_w} T_w^4 \right)$$

where $\varepsilon_e = \varepsilon_w / [1 - (1 - \varepsilon_w)(1 - \varepsilon_r^{T_w})]$ is an effective emissivity coefficient of the wall, ε_w is an emissivity coefficient of the wall material, $\varepsilon_r^{T_\infty}$ is an emissivity coefficient of the reaction products at temperature T_∞, and $\varepsilon_r^{T_w}$ is an emissivity coefficient of the reaction products at temperature T_w.

Emissivity coefficients of reaction products at specific temperature T are estimated using correlations given in [9] (also described in [3]).

Boundary layer cooling

The analysis method for estimation of a boundary layer cooling effectiveness is developed under the following assumptions:

- the large-scale distribution of mixture composition and the gas properties in the shear flow are conserved along the nozzle $(H_b = const)$;
- the convective heat flux to the wall is completely defined by the heat transfer between the wall and the boundary layer;
- the boundary layer is transparent for the radiation heat transfer.

To calculate the convective heat flux from the boundary layer to the wall, the Ievlev's correlation for similar conditions is used ([6],[9]):

$$\frac{q^{(1)}}{q^{(2)}} = \frac{S^{(1)}}{S^{(2)}}$$

where

$$S = \frac{(I_\infty^0 - I_w) T_e^{0.425} \mu_{1000}^{0.15}}{R_{1500}^{0.425} (T_e + T_w)^{0.595} (3T_e + T_w)^{0.15}}$$

Using these correlation, the heat flux is calculated as follows:

1. Calculate the heat flux $q^{(1)}$ to the wall from the core flow (that is, without taking into account the presence of the cooler boundary layer).
2. Calculate the value $S^{(1)}$ for the gas in the flow core.
3. For the known mixture composition within the boundary layer, obtain the parameters of the gas in this layer, using the chemical equilibrium composition module of the RPA.
4. Calculate the value $S^{(2)}$ for the gas in the boundary layer.
5. Calculate the corrected heat flux as
$$q^{(2)} = q^{(1)} \frac{S^{(2)}}{S^{(1)}}$$

Film cooling: gaseous film

After injecting into the thrust chamber, the gaseous coolant is mixing with existing boundary layer changing the mixture composition within this layer upstream of the injection point.

Correlations for the turbulent mixing are derived from [6] and given by

$$(r_i)_b = k_{bb} (r_i)_b^0 + k_{bf} (r_i)_f^0 \qquad (i = 0 \ldots \mathrm{NS})$$

$$(r_i)_f = k_{fb} (r_i)_b^0 + k_{ff} (r_i)_f^0 \qquad (i = 0 \ldots \mathrm{NS})$$

$$k_{bb} = \frac{\bar{m}_b^0}{\bar{m}_b}\left(1 - \frac{\xi}{2}\right) \quad , \quad k_{bf} = \frac{\bar{m}_f^0}{\bar{m}_b}\frac{\xi}{2}$$

$$k_{ff} = \frac{\bar{m}_f^0}{\bar{m}_f}\left(1 - \frac{\xi}{2}\right) \quad , \quad k_{fb} = \frac{\bar{m}_b^0}{\bar{m}_f}\frac{\xi}{2}$$

$$\bar{m}_b = \bar{m}_b^0\left(1 - \frac{\xi}{2}\right) + \bar{m}_f^0\frac{\xi}{2} \quad , \quad \bar{m}_f = \bar{m}_b^0\frac{\xi}{2} + \bar{m}_f^0\left(1 - \frac{\xi}{2}\right)$$

$$\xi = 1 - e^{-M\bar{x}^2} \quad , \quad M = K_t \bar{m}_b / \bar{m}_f$$

$$\bar{x}^2 = x / H_b$$

where r_i is a mass ratio of the species i in the mixture, NS is a total number of species within the boundary layer and the film (the initial composition of the coolant may differ from the initial composition of the boundary layer), $\bar{m}_{b,f} = \dot{m}_{b,f} / \dot{m}$ is a relative mass flow rate, $\dot{m}_f$ is mass flow rate of the coolant in the film, $\dot{m}_b$ is a mass flow rate of the gas in the boundary layer, $\dot{m}$ is total mass flow rate through the chamber, x is a distance from the location of the film injection, H_b is a thickness of the boundary layer, $K_t = (0.05 \ldots 0.20) \cdot 10^{-2}$ is a coefficient that reflects the intensity of the turbulent mixing.

Superscript *"0"* denotes the initial parameters of the boundary layer and the film at the location of injection.

Subscripts *"b"* and *"f"* denote the parameters of the boundary layer and the film correspondingly.

The mixture composition within the boundary layer is determined via a space-marching technique starting from the location of coolant injection ($\xi = 0$) to the location where the coolant is completely mixed with the boundary layer ($\xi = 1$).

Parameter H_b is defined by user and is essential for the analysis. The default value is $H_b = 0.025\, d$ where d is a diameter of the chamber at current location.

The estimation of the cooling effectiveness at each station is performed using Ievlev's correlation for similar conditions, as described in section *"Boundary layer cooling"*.

Film cooling: liquid film

When injected into the thrust chamber, the liquid coolant transformation goes through 3 phases:

Heating

Assuming that the thin liquid coolant film is transparent for the radiation heat transfer, the only component of the total heat flux reaching the wall is the radiation heat flux, whereas the convective component heats the liquid coolant. Therefore the convective heat transfer from the

liquid coolant to the wall may be neglected.

The heating equation is given by

$$dT_f = \frac{2\pi r q_w^{T_f}}{\eta \dot{m}_f \bar{c}_f} dx$$

where dT_f is an increase in temperature of the coolant, $q_w^{T_f}$ is a convective heat flux to the liquid coolant film at the coolant temperature T_f, $\dot{m}_f$ is a mass flow rate of the liquid coolant in the film, $\bar{c}_f$ is an average specific heat of the coolant, r and dx are radius and length of the current chamber segment correspondingly.

Coefficient η reflects the stability of the liquid film [6] and depends on Reynolds number calculated from the parameters of the liquid film as:

$$\mathrm{Re}_f = \frac{\dot{m}_f}{2\pi r \mu_f}$$

The heating of the film coolant is determined via a space-marching technique starting from the location of coolant injection to the location where the coolant is heated up to the temperature of vaporization or decomposition.

Vaporization

After heating up to vaporization/decomposition temperature, the part or all liquid in the film is vaporized. Similar to the heating, the convective heat transfer from the liquid coolant to the wall may be neglected.

The vaporization rate of the coolant is given by equation:

$$d\dot{m}_f = \frac{2\pi r q_w^{T_{vap}}}{Q_{vap}} dx$$

where $d\dot{m}_f$ is a rate of the coolant vaporization or decomposition, $\dot{m}_f$ is a mass flow rate of the coolant in the film, $q_w^{T_{vap}}$ is a convective heat flux to the liquid coolant film at the coolant vaporization temperature T_{vap}, Q_{vap} is a coolant heat of vaporization or decomposition, r and dx are radius and length of the current chamber segment correspondingly.

The vaporization or decomposition of the film coolant is determined via a space-marching technique starting from the location where the coolant reaches the temperature of vaporization or decomposition, to the location where the whole coolant is completely vaporized or decomposed.

Mixing with boundary layer

The gaseous products of vaporization/decomposition are mixing with existing boundary layer, producing the layer with new mixture composition. The mixing itself and the estimation of the boundary layer cooling effectiveness is performed as described in sections *"Film cooling: gaseous film"* and *"Boundary layer cooling"*.

Radiation cooling

The steady-state heat transfer for the radiation cooled station of the thrust chamber is given by:

$$q_w^{T_{wg}} + q_r^{T_{wg}} = \frac{\lambda_w}{t_w}(T_{wg} - T_{wc}) = \varepsilon_{wc}\sigma T_{wc}^4 = q_{rc}^{T_{wc}}$$

where $q_w^{T_{wg}}$ and $q_r^{T_{wg}}$ are convective and radiation heat flux to the inner surface of the wall at the temperature T_{wg}, $q_{rc}^{T_{wc}}$ is a radiation heat flux from the outer surface of the wall at the temperature T_{wc}, T_{wg} is a temperature on the inner surface of the wall, T_{wc} is a temperature on the outer surface of the wall, ε_{wc} is an emissivity coefficient of the wall material, λ_w is a thermal conductivity of the wall at the temperature $T = 0.5(T_{wg} + T_{wc})$, t_w is a thickness of the wall.

The steady-state heat transfer at each chamber/nozzle station is solved iteratively and finishes when both T_{wg} and T_{wc} are found such that the heat flux to the inner surface of the wall $(q_w^{T_{wg}} + q_r^{T_{wg}})$ is equal to the heat flux from the outer surface $q_{rc}^{T_{wc}}$.

Regenerative cooling

At each station of thrust chamber, the following set of equations is used to determine the temperature of the wall and the coolant:

$$(q_w^{T_{wg}} + q_r^{T_{wg}}) A_w = \dot{m}_c \bar{c}_c (T_c^{\mathrm{out}} - T_c^{\mathrm{in}})$$

$$dT_c = \frac{2\pi R (q_w^{T_{wg}} + q_r^{T_{wg}})}{\dot{m}_c \bar{c}_c} dx$$

$$q_w^{T_{wg}} + q_r^{T_{wg}} = \frac{\lambda_w}{t_w}(T_{wg} - T_{wc})$$

$$q_w^{T_{wg}} + q_r^{T_{wg}} = \alpha_c (T_{wc} - T_c) = q_{wc}^{T_{wc}}$$

$$\alpha_c = \eta_r Nu \frac{\lambda_c}{d_e}$$

$Nu = 0.021 \mathrm{Re}_c^{0.8} Pr_c^{0.4} \left(0.64 + 0.36 \frac{T_c}{T_{wc}}\right)$ (for kerosene) [6]

$Nu = 0.033 \mathrm{Re}_c^{0.8} Pr_c^{0.4} \left(\frac{T_c}{T_{wc}}\right)^{0.57}$ (for liquid hydrogen) [9]

$Nu = 0.0185 \mathrm{Re}_c^{0.8} Pr_c^{0.4} \left(\frac{T_c}{T_{wc}}\right)^{0.1}$ (for methane) [9]

$Nu = 0.023 \mathrm{Re}_c^{0.8} Pr_c^{0.4}$ (for other coolants) [6]

where $q_w^{T_{wg}}$ and $q_r^{T_{wg}}$ are convective and

radiation heat flux to the inner surface of the wall at the temperature T_{wg} , T_{wg} is a gas-side wall temperature, T_{wc} is a coolant-side wall temperature, λ_w is a thermal conductivity of the chamber wall at the temperature $T=0.5(T_{wg}+T_{wc})$, t_w is a thickness of the chamber wall, T_c is an average coolant temperature, T_c^{in} is an initial temperature of the coolant as it enters the station, T_c^{out} is a final temperature of the coolant as it leaves the station, $\bar{c}_c$ is an average coolant specific heat, $\dot{m}$ is coolant mass flow rate, A_w is a wall surface area, $d_e=4A/\Pi$ is an equivalent diameter of the cooling passage, A is a total cross-section area of the cooling passages (that is the sum of the cross-sections of all passages at specific station), Π is a total perimeter of the cooling passages (that is the sum of the perimeters of all passages at specific station), η_f is a coefficient, introduced to reflect the increase in surface area of the cooling passages (fin effect).

Pressure drop in cooling passages is calculated from

$$\Delta p=\lambda\frac{l}{d_e}\rho\frac{w^2}{2}$$

where l is a length of the cooling passage, d_e is an equivalent diameter of the cooling passage, ρ is an average density of the coolant in the segment, $w=\dot{m}/\rho A$ is a coolant flow velocity, $\dot{m}$ is a coolant total mass flow rate.

Friction loss coefficient λ is obtained from following correlations [10]:

- for laminar flows (Re ≤ 2320): $\lambda=\frac{64}{\mathrm{Re}}\varepsilon_f$
- for turbulent flows (2320 < Re < 10^5): $\lambda=\frac{0.3164}{\sqrt[4]{\mathrm{Re}}}\varepsilon_f$
- for turbulent flows (Re > 10^5): $\lambda=\left(0.0032+\frac{0.221}{\mathrm{Re}^{0.237}}\right)\varepsilon_f$

Coefficients η_r and ε_f depend on geometric shape of the coolant passages (coaxial shells, welded tubes, or milled channels) and obtained as described in [3].

Thermal barrier coating (TBC)

For the analysis of thrust chambers with TBC the following steady-state equation for heat transfer through the wall is used:

$$q_w^{T_{wg}}+q_r^{T_{wg}} = \frac{1}{\left[\frac{t_1}{\lambda_1}+\frac{t_2}{\lambda_2}+\ldots+\frac{t_N}{\lambda_N}\right]}\ (T_{wg}-T_{wc})$$

where $t_1, t_2, \ldots, t_N$ are thicknesses of TBC layers (1...N-1) and the base wall (N), $\lambda_1, \lambda_2, \ldots, \lambda_N$ are thermal conductivities of TBC layers (1...N-1) and the base wall (N).

Procedure of thermal analysis

The parameters of the heat transfer and cooling are determined iteratively via an space-marching technique. At each iteration step the program marches axially from the first station of the thrust chamber to the last one, obtaining the parameters for each station. For each station, the convergence criteria is calculated as

$$\delta=\frac{|T_{wg}^{(i-1)}-T_{wg}^{(i)}|}{T_{wg}^{(i-1)}} < 0.05\,T_{wg}^{(i-1)}$$

where $T_{wg}^{(i-1)}$, $T_{wg}^{(i)}$ are gas-side wall temperature at previous and current iteration steps correspondingly.

The iteration continues until the convergence is achieved at all stations.

Reaction products at any station of thrust chamber, both in the core flow and in the boundary layer, and their thermodynamic and transport properties are obtained from thermodynamic analysis.

Engine cycle analysis and dry mass estimation

Engine cycle analysis and weight estimation module is capable of analyzing the operational characteristics of numerous engine configurations, performing a power balance of the turbomachinery to achieve a required combustion chamber pressure.

In the current version, the supported the following cycles:

- staged-combustion (SC),
- full-flow staged-combustion (FFSC),
- gas-generator (GG).

All cycles allow variations of the flow diagram including the number of combustion devices (gas generator or preburner), the number of turbopumps, arrangement of turbines (serial or parallel), availability of booster pumps, availability of kick pumps, availability of tap-off branches.

Top-level parameters include:

- type of combustion devices:
  - oxidizer-rich
  - fuel-rich
- number of independent turbopumps,
- number of gas generators/preburners.

The program implements an approach based on

flow path analysis, which requires the propellant feed system flow diagram is clearly defined, and the set of parameters for each component of flow diagram is specified.

The current version of the program is capable of obtaining the operational parameters of the whole feed system, but some parameters of its components have to be specified by the user, including:

- efficiency of pumps and turbines,
- pressure drop in valves, injectors, cooling jackets,
- temperature in combustion device (gas generator or preburner) which is usually is limited by properties of used construction materials,
- turbines pressure ratios (only for supplementary turbines and main turbine in GG cycle).

These parameters may be specified using either available data on historic engines, or recommendations derived from analysis of such data [12].

The flow diagram is manually decomposed into several sub-systems:

- *component (fuel and oxidizer) feed subsystems*, which begin at component inlet and end at injectors of combustion chamber and/or combustion device (GG or preburner), and include booster pumps, main pumps, kick pumps, supplementary turbines, valves, cooling jackets, injectors, and sub-branches;
- *power subsystems*, which begin at combustion device (GG or preburner) and end either at injector of thrust chamber (in SC and FFSC cycles) or at exhaust nozzle (in GG cycle), and include combustion device, gas ducts, turbines, injector (in SC and FFSC cycles) and nozzle (in GG cycle).

An example of decomposition of is flow diagram of staged-combustion cycle is shown in Fig.3.

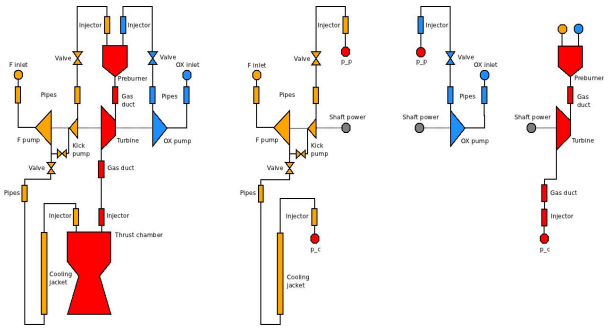

Fig. 3: Flow diagram of oxidizer-rich SC cycle (left) and its decomposition into fuel feed, oxidizer feed, and power subsystems

The program implements the iterative procedure to achieve the following goals:

- *for gas-generator cycle*: for given thrust chamber pressure, find such a mass flow rate through the turbines that the power of turbines with specified pressure ratios is sufficient for developing the required discharge pressure of pumps;
- *for staged-combustion cycle*: for given thrust chamber pressure, find such a pressure in preburners and turbine pressure ratios that for specified temperature in preburners the power of turbines is sufficient for developing the required discharge pressure of pumps.

The pump shaft power is given by

$$N_p = \frac{\dot{m}}{\eta_p}\frac{(p_{out}-p_{\text{in}})}{\rho}$$

where η_p is a pump overall efficiency.

The power developed by gas turbine is given by

$$N_t = \dot{m}_t \eta_t \frac{\gamma}{\gamma-1} R^0 T^0_{\text{t in}}\left[1-\left(\frac{1}{\delta_t}\right)^{\frac{\gamma-1}{\gamma}}\right]$$

where η_t is turbine overall efficiency, R^0 is stagnation gas constant, $T^0_{\text{t in}}$ is turbine inlet stagnation temperature, $\delta_t = p^*_{\text{t in}}/p_{\text{t out}}$ is turbine pressure ratio, $p^*_{\text{t in}}$ is turbine inlet stagnation pressure, $p_{\text{t out}}$ is turbine discharge pressure.

The power developed by hydraulic turbine is given by

$$N_t = \dot{m}_t \eta_t \frac{(p_{out}-p_{\text{in}})}{\rho}$$

where p_{in} is turbine inlet pressure, p_{out} is turbine discharge pressure.

For given temperature in gas generator or preburner, the parameters of combustion products are obtained from thermodynamic analysis.

When using gas-generator cycle, the program estimates the overall engine performance taking into account the mass flow rate through turbine.

The engine dry mass is assessed using semi-empirical relations for each major type of engines, derived from [13].

Development tools

Development tools are available, allowing the user to create various custom solutions, including simple scripts written in JavaScript, programs written in Python, or complex applications written in C++.

Besides rocket propulsion analysis, the following thermodynamic problems can be solved:

(p,T)=const, *(p,I)=const*, *(p,S)=const*, *(V,T)=const*, *(V,U)=const*, and *(V,S)=const*.

Application examples

Thermodynamics

Comparison with a commonly used NASA equilibrium program CEA [4],[5] has been performed for a large number of test cases. Some of them are listed in the Table 1.

Table 1: Selected test cases

Parameter	Case #1	Case #2	Case #3
Chamber pressure, MPa	10	10	5
Oxidize	LOX	LOX	N2O4
Fuel	LH2	RP-1	UDMH
O/F	6.0	2.6	2.6

A perfect agreement is obtained between the CEA and PRA programs. Any percent differences in parameter values are in at least the third decimal place and are negligible (see Table 2).

Table 2: Comparison of test cases

Parameter	Test case #1			Test case #2			Test case #3		
	CEA	RPA	δ, %	CEA	RPA	δ, %	CEA	RPA	δ, %
T, K	3523.79	3523.79	0.0	3723.63	3723.63	0.0	3392.31	3392.31	0.0
I, kJ/kg	-986.31	-986.31	0.0	-784.21	-784.21	0.0	88.271	88.271	0.0
S, kJ/(kg K)	17613	17.613	0.0	11127	11.127	0.0	11149	11.149	0.0
M	13.513	13.513	0.0	23.603	23.603	0.0	23.524	23.524	0.0
Cp, kJ/(kg K)	8.2367	8.2367	0.0	6026	6.026	0.0	5.2960	5.296	0.0
γ	1.1425	1.1425	0.0	1.1392	1.1392	0.0	1.1385	1.1385	0.0
a, m/s	1574.0	1573.95	0.0	1222.4	1222.4	0.0	1168.4	1168.34	0.0
ρ, kg/m^3	4.612	4.612	0.0	7.6236	7.6237	0.001	4.1701	4.1702	0.002

Performance analysis

This examples show the RPA capability concerning predicting the performance of rocket engines compared with available data on historic engines RD-170, RD-275, and RS-25 (SSME).

Table 3: Comparison of actual and predicted engine performance

Parameter	RD-170			RD-275			RS-25 (SSME)		
	Actual	RPA	δ, %	Actual	RPA	δ, %	Actual	RPA	δ, %
Isp (vac), s	337	337.8	0.2	316	314.7	0.4	452	449.5	0.5
Isp (SL), s	309	308.7	0.0	287	282.2	1.3	366	367.9	0.5

An excellent agreement is obtained between the actual performance and performance predicted by RPA program.

The comparison of ideal performance predicted by RPA with ideal performance calculated by NASA CEA code (not presented in this paper) provides an excellent agreement as well.

Thermal analysis: SSME 40k

This example shows the RPA capability concerning thermal analysis.

The comparison between available reference for SSME 40k [14] and RPA prediction has been performed.

The obtained agreement between the RPA prediction and referenced data is sufficient for the tool used in conceptual and preliminary design.

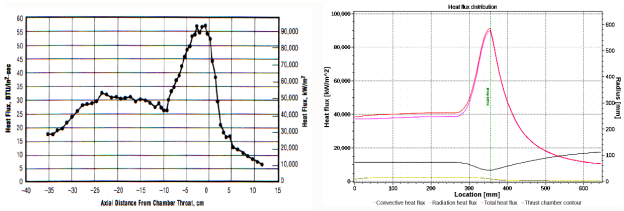

Fig. 4: SSME 40 K calorimeter chamber heat flux profile [14] (left) and predicted by RPA (right)

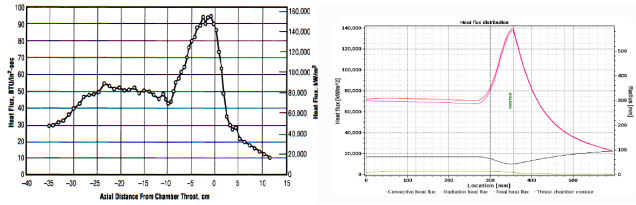

Fig. 5: SSME 40 K regenerative chamber predicted heat flux profile [14] (left) and predicted by RPA (right)

Quantitative and qualitative differences in results are explained by the following factors:

- RPA does not simulate fuel atomization and dispersion, as well as droplets burning;
- the hot gas properties for thermal analysis are retrieved from quasi one-dimensional flow model;
- the heat transfer is simulated in RPA using semi-empirical relations.

Cycle analysis and dry mass estimation

In its current implementation, the cycle analysis requires that the pressure drop in a hydraulic components and efficiencies of the pumps and turbines are specified by the user. Therefore it is essential for the reliable result to provide accurate input data.

This examples show the capability of RPA concerning predicting the parameters of the propellant feed system compared with available data on historic staged-combustion engine RD-170 [15].

Table 4: Comparison of actual and predicted cycle parameters

Parameter	Actual [15]	RPA [16]	δ, %
Preburner pressure, MPa	53.5	51.0	4.67
Preburner mass flow rate, kg/s	2 x 836 = 1672	1767.8	5.73
Turbine pressure ratio	1.94	2.04	5.15
Turbine shaft power, MW	191.9	184.4	3.91
Oxidizer main pump discharge pressure, MPa	60.2	64.1	6.48
Oxidizer main pump shaft power, MW	130.9	125.6	4.05

Parameter	Actual [15]	RPA [16]	δ, %
Fuel main pump discharge pressure, MPa	50.6	49.3	2.57
Fuel main pump shaft power, MW	57.9	57.8	0.01
Dry engine mass, kg	9500	9591	0.95

The obtained good agreement between the RPA prediction and referenced data is sufficient for the tool used in conceptual and preliminary design.

Further examples

Further examples are available within RPA distribution package and online at www.propulsion-analysis.com

Conclusion

The most important aspects of the physical models implemented in RPA were described. The results of validation were presented. The obtained agreement between the RPA prediction and referenced data is sufficient for the tool used in conceptual and preliminary design studies.

Further development of the tool will include:

- design of thrust optimized nozzle contour (TOC),
- improved options for thermal analysis (e.g., option to jackets with bi-directional channels, option to introduce BLC formed by injector),
- improved options for modeling feed systems (e.g. estimation of pressure drop in a hydraulic components and efficiencies of the pumps and turbines),
- better integration of different modules.

Nomenclature

A – area, m^2
C_f – thrust coefficient
d – diameter, m
I – enthalpy, J/kg
I_{sp} – specific impulse
L, l – length, m
M – Mach number
$\dot{m}$ – mass flow rate, kg/s
N – power, N
Π – perimeter, m
p – pressure, Pa
q – heat flux, W/m^2
ρ – density, kg/m^3
R – gas constant, J/(kg·K)
r – radius, m
S – entropy, J/(kg·K)
T – temperature, K
t – thickness, m
w – velocity, m/s
λ – characteristic Mach number or thermal conductivity, W/(m·K)
γ – specific heat ratio
$\sigma = 5.670373 \times 10^{-8}$ – Stefan–Boltzmann constant, W/(m^2·K^4)

Superscripts

0 – stagnation flow parameter

Subscripts

c – chamber or coolant
e – nozzle exit
in – inlet
out – outlet, discharge
p – pump
t – throat or turbine
w – wall
wg – wall gas side
wc – wall coolant side
∞ – core flow

References

1. Ponomarenko, A. RPA: Design Tool for Liquid Rocket Engine Analysis. May 2010.
2. Ponomarenko, A. RPA: Tool for Rocket Propulsion Analysis. Assessment of Delivered Performance of Thrust Chamber. March 2013.
3. Ponomarenko, A. RPA: Tool for Rocket Propulsion Analysis. Thermal Analysis of Thrust Chambers. June 2012.
4. Gordon, S. and McBride, B.J. Computer Program for Calculation of Complex Chemical Equilibrium Compositions and Applications I. Analysis. NASA RP-1311, Oct. 1994.
5. Gordon, S. and McBride, B.J. Computer Program for Calculation of Complex Chemical Equilibrium Compositions and Applications II. User's Manual and Program Description. NASA RP-1311-P2, June 1996.
6. Vasiliev A.P., Kudryavtsev V.M. et al. Basics of theory and analysis of liquid-propellant rocket engines, vol.2. 4th Edition. Moscow, Vyschaja Schkola, 1993.
7. Alemasov V.E., Dregalin A.F., Tishin A.P. Theory of Rocket Engines. Moscow, Mashinostroenie, 1980.
8. Huzel, D.K., Hwang, D.H., Modern Engineering for Design of Liquid Rocket Engines. American Institute of Aeronautics and Astronautics, 1992.
9. Lebedinsky E.V., Kalmykov G.P., et al. Working processes in liquid-propellant rocket engine and their simulation. Moscow, Mashinostroenie, 2008.
10. Katorgin B.I., Kiselev A.S., Sternin L.E., Chvanov V.K. Applied gas dynamics. Moscow, Vusovskaja kniga, 2009.
11. Dobrovolsky M.B. Liquid-propellant rocket engines. 2nd Edition. Moscow, Bauman MSTU, 2005.

12. Configuring and Running Rocket Engine Cycle Analysis with RPA Standard 2.1. http://www.propulsion-analysis.com

13. Kozlov A.A., Novilov V.N., Solovjev E.V. Feed and control systems of liquid-propellant rocket plants. Moscow, Mashinostroenie, 1988.

14. Carol E. Dexter, Mark F. Fisher, James R. Hulka, Konstantin P. Denisov, Alexander A. Shibanov, and Anatoliy F. Agarkov. Scaling Techniques for Design, Development, and Test. Liquid Rocket Thrust Chambers - Aspects of Modeling, Analysis, and Design - Progress in Astronautics and Aeronautics, Volume 200.

15. Sutton, G.P. and Biblarz, O. Rocket Propulsion Elements, 7th Edition. John Wiley & Sons, 2001.

16. Configuration file “examples/cycle_analysis/RD-170.cfg” from distribution package of RPA.